

Real tropical hyperfaces by patchworking in polymake

Michael Joswig^{1,2} and Paul Vater²

¹ TU Berlin, Chair of Discrete Mathematics/Geometry

² MPI MiS Leipzig

joswig@math.tu-berlin.de, vater@mis.mpg.de,

Keywords: Hilbert’s 16th problem; real algebraic hypersurfaces; Viro’s patchworking; tropical hypersurfaces

1 Introduction

Hilbert’s 16th problem asks about topological constraints for real algebraic hypersurfaces in projective space. In the 1980s Viro developed patchworking as a combinatorial method to construct real algebraic hypersurfaces with unusually large \mathbb{Z}_2 -Betti numbers [14,15,16,17]. A major breakthrough of this idea was Itenberg’s refutation of Ragsdale’s Conjecture [9]. Today patchworking is most naturally interpreted within the larger framework of tropical geometry [12]. In this way patchworking is a combinatorial avenue to real tropical hypersurfaces.

Here we report on a recent implementation of patchworking and real tropical hypersurfaces in `polymake` [1], version 4.1 of April 2020. The first software for patchworking that we are aware of is the “Combinatorial Patchworking Tool” [4], which works web-based and is restricted to the planar case. A second implementation is `Viro.sage` [18] which is capable of patchworking in arbitrary dimension and degree. Our implementation has the same scope as `Viro.sage` but it is superior in two ways. First, it naturally ties in with a comprehensive hierarchy of polyhedral objects in `polymake`; e.g., this allows for a rich choice of constructions of real tropical hypersurfaces. Second, our implementation is more efficient. This is demonstrated by several experiments with curves and surfaces of various degrees. As a new mathematical contribution we provide a census of Betti numbers of real tropical surfaces.

Acknowledgments. We are indebted to Ilia Itenberg, Johannes Rau and Kristin Shaw for valuable comments on a previous version of this text. Moreover, we are grateful to Lars Kastner and Benjamin Lorenz for helping with the experiments. M. Joswig has been supported by DFG (EXC 2046: “MATH+”, SFB-TRR 195: “Symbolic Tools in Mathematics and their Application”, and GRK 2434: “Facets of Complexity”).

1.1 Tropical hypersurfaces in \mathbb{TP}^{n-1}

Let $f = \bigoplus_{v \in V} c_v \odot x^v \in \mathbb{T}[x_1, \dots, x_n]$ be a tropical polynomial where V is a finite subset of \mathbb{Z}^n . We use the multi-index notation $x^v = x_1^{v_1} \cdots x_n^{v_n}$, and

$\mathbb{T} = \mathbb{R} \cup \{\infty\}$, $\oplus = \min$ and $\odot = +$. The *tropical hypersurface* $\mathcal{T}(f)$ is the tropical vanishing locus of f , i.e., the set of points in \mathbb{R}^n , where the minimum of the evaluation function $x \mapsto f(x)$ is attained at least twice. Throughout we will assume that f is homogeneous of degree d , i.e., for each $v \in V$ we have $v_1 + \dots + v_n = d$. In that case $\mathcal{T}(f)$ descends to the *tropical projective torus* $\mathbb{R}^n/\mathbb{R}\mathbf{1}$, where $\mathbf{1} = (1, \dots, 1)$. The *Newton polytope* of f is $\mathcal{N}(f) = \text{conv } V$, and the coefficients of f induce a regular subdivision, $\mathcal{S}(f)$. The latter is dual to $\mathcal{T}(f)$. We refer to [12] and [3] for further details.

The tropical projective space $\mathbb{TP}^{n-1} = (\mathbb{T}^n - \{\infty\mathbf{1}\})/\mathbb{R}\mathbf{1}$ compactifies $\mathbb{R}^n/\mathbb{R}\mathbf{1}$. It is naturally stratified into lower dimensional tropical projective tori, marked by those coordinates which are finite. In this way the pair $(\mathbb{TP}^{n-1}, \mathbb{R}^n/\mathbb{R}\mathbf{1})$ is naturally homeomorphic with an $(n-1)$ -simplex and its interior. Often we will identify the tropical hypersurface $\mathcal{T}(f)$ with its compactification in \mathbb{TP}^{n-1} .

1.2 Viro's patchworking

The following is essentially a condensed version of [13, §3.1], with minor variations. A *sign distribution* $\epsilon \in \mathbb{Z}_2^V$ can be *symmetrized* to the function

$$s_\epsilon : \mathbb{Z}_2^n \rightarrow \mathbb{Z}_2^V, \quad s_\epsilon(z)(v) := \epsilon(v) + \langle z, v \rangle \pmod{2} .$$

As in [6] we choose our signs in $\mathbb{Z}_2 = \{0, 1\}$, which corresponds to ± 1 via $z \mapsto (-1)^z$. Further, the elements $z \in \mathbb{Z}_2^n$ are in bijection with the 2^n orthants of \mathbb{R}^n via $z \mapsto \text{pos}\{(-1)^{z_1}e_1, \dots, (-1)^{z_n}e_n\}$, where e_1, \dots, e_n are the standard basis vectors of \mathbb{R}^n , and $\text{pos}(\cdot)$ denotes the nonnegative hull. We will use this identification throughout and, consequently, we call z itself an *orthant*.

The tropical hypersurface $\mathcal{T}(f)$ is a polyhedral complex in \mathbb{TP}^{n-1} , and its k -dimensional cells are dual to the $(n-1-k)$ -cells of $\mathcal{S}(f)$. In particular, each maximal cell F of $\mathcal{T}(f)$ corresponds to an edge, $V(F) \subset V$, of $\mathcal{S}(f)$. We write \mathcal{T}_{n-2} for the set of maximal cells (which are $(n-2)$ -dimensional polyhedra) and denote powersets as $\mathcal{P}(\cdot)$.

Note that there are no $(n-2)$ -cells of $\mathcal{T}(f)$ in the boundary $\mathbb{TP}^{n-1} - \mathbb{R}^n/\mathbb{R}\mathbf{1}$. The *real phase structure* on $\mathcal{T}(f)$ induced by ϵ is the map

$$\phi_\epsilon : \mathcal{T}_{n-2} \rightarrow \mathcal{P}(\mathbb{Z}_2^n), \quad F \mapsto \{z \in \mathbb{Z}_2^n \mid s_\epsilon(z)(v) \neq s_\epsilon(z)(w)\} \text{ for } \{v, w\} = V(F) .$$

That is, for each maximal cell F of $\mathcal{T}(f)$ this describes the set of orthants, in which the symmetrized sign distribution takes distinct values on the two vertices of the dual edge $V(F)$ in $\mathcal{S}(f)$. This extends to all cells G of $\mathcal{T}(f)$ by setting $\phi_\epsilon(G) := \bigcup \phi_\epsilon(F)$, where the union is taken over all maximal cells $F \in \mathcal{T}_{n-2}$ containing G . The pair $\mathcal{T}_\epsilon(f) = (\mathcal{T}(f), \epsilon)$ is a *real tropical hypersurface*.

Let \bar{z} , defined by $\bar{z}_i = 1 - z_i$, be the *antipode* of $z \in \mathbb{Z}_2^n$. We define an equivalence relation \sim on $\mathbb{Z}_2^n \times \mathbb{TP}^{n-1}$, which identifies copies of \mathbb{TP}^{n-1} along common strata, by letting

$$(z, x) \sim (z', y) : \iff x = y \text{ and } (\bar{z} = z' \text{ or } (x_i = \infty = y_i \iff z_i = 1 = z'_i)) .$$

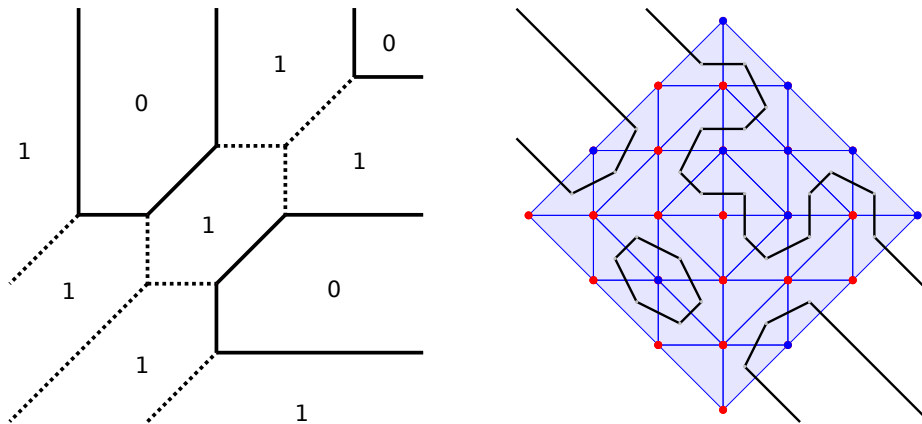


Fig. 1. Real tropical elliptic curve (left) and its real part (right)

This identifies $\{z\} \times \mathbb{TP}^{n-1}$ and $\{\bar{z}\} \times \mathbb{TP}^{n-1}$ one to one for each z . It follows that the quotient $(\mathbb{Z}_2^n \times \mathbb{TP}^{n-1})/\sim$ is homeomorphic to the real projective space \mathbb{RP}^{n-1} . Combinatorially that construction can be seen as follows: the union of the 2^n simplices $\text{conv}\{(-1)^{z_1}e_1, \dots, (-1)^{z_n}e_n\}$, where z ranges over all orthants, gives the boundary of the regular cross polytope $\text{conv}\{\pm e_1, \dots, \pm e_n\}$ in \mathbb{R}^n . Taking the quotient modulo antipodes yields \mathbb{RP}^{n-1} .

The *real part* of the real tropical hypersurface $\mathcal{T}_\epsilon(f) = (\mathcal{T}(f), \epsilon)$, denoted $\mathbb{RT}_\epsilon(f)$, is now defined as the collection of polyhedral complexes in $\mathbb{Z}_2^n \times \mathbb{TP}^{n-1}$ consisting of the polyhedra

$$\{\{z\} \times F \mid F \in \mathcal{T}_{n-2} \text{ and } z \in \phi_\epsilon(F)\}$$

and their faces. Note that $\{z\} \times F \in \mathbb{RT}_\epsilon(f)$ if and only if $\{\bar{z}\} \times F \in \mathbb{RT}_\epsilon(f)$, and hence we may restrict to the part of $\mathbb{RT}_\epsilon(f)$ in $(\{0\} \times \mathbb{Z}_2^{n-1}) \times \mathbb{TP}^{n-1}$.

To avoid cumbersome notation and language we call the quotient of $\mathbb{RT}_\epsilon(f)$ by \sim also the *real part* of $\mathcal{T}_\epsilon(f)$ and use the same symbol, $\mathbb{RT}_\epsilon(f)$. In this way $\mathbb{RT}_\epsilon(f)$ becomes a piecewise linear hypersurface in $\mathbb{RP}^{n-1} \approx \mathbb{Z}_2^n \times \mathbb{TP}^{n-1}/\sim$.

The above construction is relevant for its connection with real algebraic geometry. To simplify the exposition we now consider a special case: Setting $\Delta_{n-1} = \text{conv}\{e_1, \dots, e_n\}$, we assume that the set $V = d \cdot \Delta_{n-1} \cap \mathbb{Z}^n$ is the set of lattice points in the dilated unit simplex. This entails that the projective toric variety generated from V is the (complex) projective space \mathbb{CP}^{n-1} . The following result comes in various guises; this version occurs in [15] and [8, Proposition 2.6].

Theorem 1 (Viro's combinatorial patchworking theorem). *Let f be a homogeneous tropical polynomial of degree d with support $V = d \cdot \Delta_{n-1} \cap \mathbb{Z}^n$. Then, for each sign distribution $\epsilon \in \mathbb{Z}_2^n$, there exists a nonsingular real algebraic hypersurface X in \mathbb{CP}^{n-1} , also with Newton polytope $\mathcal{N}(f) = d \cdot \Delta_{n-1}$, such that*

$$(\mathbb{Z}_2^n \times \mathbb{TP}^{n-1}/\sim, \mathbb{RT}_\epsilon(f)) \text{ is } \mathbb{Z}_2\text{-homologous to } (\mathbb{RP}^{n-1}, \mathbb{R}X) .$$

If additionally $\mathcal{S}(f)$ is *unimodular*, i.e., each simplex has normalized volume one, this is “primitive patchworking”. In the primitive case stronger conclusions hold [16,13]. The notion “combinatorial patchworking” refers to the condition $\mathcal{N}(f) = d \cdot \Delta_{n-1}$. This is what our implementation supports, for arbitrary degrees and dimensions. More general results require to carefully take into account the toric geometry of $\mathcal{N}(f)$.

Example 2. With $n = d = 3$ we consider the tropical polynomial

$$f = x^3 \oplus 1x^2y \oplus 1x^2z \oplus 4xy^2 \oplus 3xyz \oplus 4xz^2 \oplus 9y^3 \oplus 7y^2z \oplus 7yz^2 \oplus 9z^3$$

in $\mathbb{T}[x, y, z]$, where we omit ‘ \odot ’ for improved readability. The tropical hypersurface $\mathcal{T}(f)$ is the tropical elliptic curve in $\mathbb{R}^3/\mathbb{R}\mathbf{1}$ in Figure 1 (left). The sign distribution $\epsilon = (0, 1, 0, 1, 1, 1, 0, 1, 1)$ yields a real tropical curve with real part in $\mathbb{Z}_2^3 \times \mathbb{TP}^2/\sim$ which has two components; cf. Figure 1 (right). This primitive patchwork corresponds to a classical Harnack curve of degree 3; cf. [9, Sec. 5].

2 Betti numbers from combinatorial patchworking

Our goal is to exhibit a census of Betti numbers of real tropical surfaces in $\mathbb{Z}_2^4 \times \mathbb{TP}^3/\sim$. Throughout the following let f be a tropical polynomial of degree d in $n = 4$ homogeneous variables; we will assume that $\mathcal{S}(f)$ is a regular and full triangulation of $V = d \cdot \Delta_3 \cap \mathbb{Z}^4$. That is, we focus on combinatorial patchworks. A triangulation of V is *full* if it uses all points in V ; a unimodular triangulation is necessarily full. While the converse holds in the plane, there are many more full triangulations of $d \cdot \Delta_3$ than unimodular ones if $d \geq 3$. Further, with

$$k := \frac{1}{6}d^3 + d^2 + \frac{11}{6}d + 1, \quad (1)$$

which is the cardinality of V , we pick a sign vector $\epsilon \in \mathbb{Z}_2^k$. This gives rise to a real algebraic surface X in \mathbb{CP}^3 whose real part $\mathbb{R}X$ is “near the tropical limit” $\mathbb{RT}_\epsilon(f)$ in the sense of [13]. Itenberg [6, Theorems 3.2/3.3] showed that the Euler characteristic satisfies

$$\chi(\mathbb{R}X) \geq \frac{4d - d^3}{3}, \quad (2)$$

with equality attained in the primitive/unimodular case. Moreover, by [6, Theorem 4.2],

$$b_1(\mathbb{R}X) \leq \frac{2d^3 - 6d^2 + 7d}{3}, \quad (3)$$

where $b_q(\cdot)$ are \mathbb{Z}_2 -Betti numbers; see also [7] for bounds without the fullness assumption. However, if $\mathcal{S}(f)$ is even unimodular then, by [6, Theorem 4.1],

$$b_0(\mathbb{R}X) \leq \binom{d-1}{3} + 1. \quad (4)$$

See Table 1 for explicit numbers in the range which is relevant for our experiments. The main result of [13] furnishes a vast generalization of (4) to arbitrary dimensions.

Table 1. Bounds for Euler characteristic and Betti numbers, depending on the degree d . The values k , χ' , b'_0 and b'_1 are the right hand sides of (1), (2), (4) and (3), respectively.

d	k	χ'	b'_0	b'_1
3	20	-5	1	7
4	35	-16	2	20
5	56	-35	5	45
6	84	-64	11	86

Example 3. The subdivision $\mathcal{S}(f)$ induced by the tropical polynomial

$$\begin{aligned} f = & 5x^3 \oplus 1x^2y \oplus 1xy^2 \oplus 5y^3 \oplus 2x^2z \oplus 0xyz \oplus 2y^2z \\ & \oplus 0xz^2 \oplus 0yz^2 \oplus 1z^3 \oplus 2x^2w \oplus 0xyw \oplus 2y^2w \oplus 1xzw \\ & \oplus 1yzw \oplus 1z^2w \oplus 3xw^2 \oplus 3yw^2 \oplus 4zw^2 \oplus 8w^3 \end{aligned}$$

is a full triangulation of $3 \cdot \Delta_3$ which is not unimodular. Its f -vector reads $(20, 60, 64, 23)$, and its automorphism group is of order 6. The sign distribution

$$\epsilon = (0, 0, 0, 0, 0, 0, 0, 1, 1, 0, 1, 1, 1, 1, 1, 0, 1, 1, 1, 0)$$

yields a real tropical surface $\mathbb{R}\mathcal{T}_\epsilon(f)$ whose real part has Betti vector $(2, 1, 2)$.

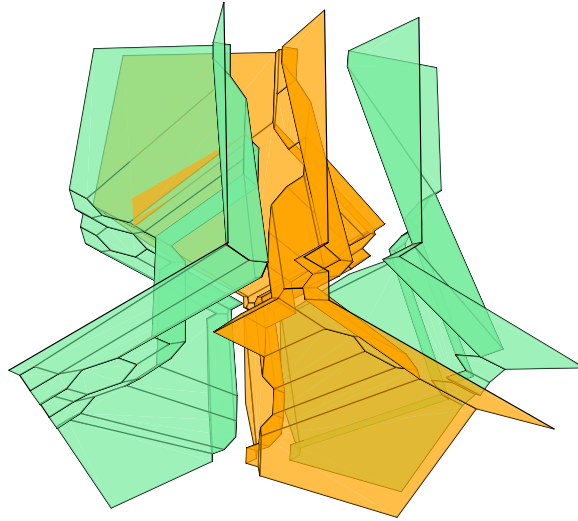


Fig. 2. The real part of a cubic surface with Betti vector $(2, 1, 2)$. There are three affine sheets, of which the outer two account for one connected component in $\mathbb{R}\mathbb{P}^3$, which is homeomorphic to \mathbb{S}^2 ; the middle sheet forms a component homeomorphic to $\mathbb{R}\mathbb{P}^2$.

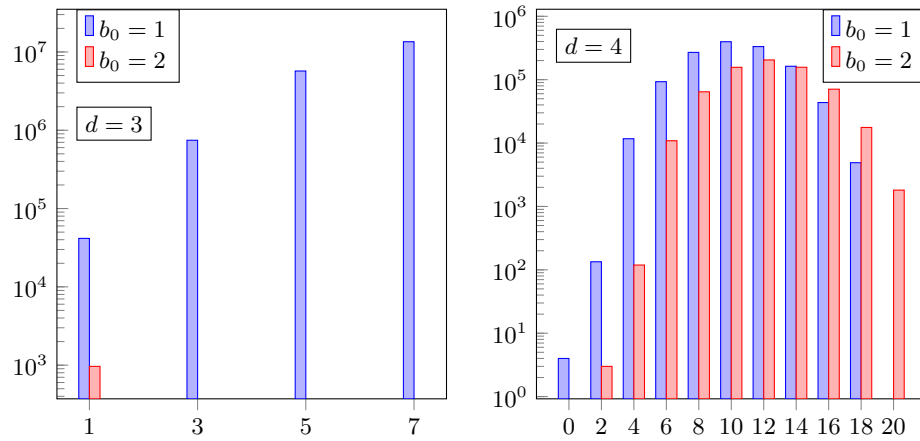


Fig. 3. Distribution of Betti vectors for surfaces of degrees 3 and 4. The colors indicate values for $b_0 = b_2$, the values on the x -axis indicate values for b_1 . For $d = 3$ the most frequent vector is $(1, 7, 1)$ with 67.52%. For $d = 4$ it is $(1, 10, 1)$ with 19.86%.

2.1 Combinatorial description of the homology

The polyhedral description of $\mathbb{R}\mathcal{T}_\epsilon(f)$ directly gives a combinatorial description of the homology; see also [13, Proposition 3.17]. The cellular chain modules read

$$C_q(\mathbb{R}\mathcal{T}_\epsilon(f); \mathbb{Z}_2) = \bigoplus_{\sigma \text{ cell of } \mathcal{T}_\epsilon(f), \dim \sigma = q} \left(\bigoplus_{z \in \phi_\epsilon(\sigma)} \mathbb{Z}_2^{\{\sigma \times \{z\}\}} \right) \quad (5)$$

and $\partial(\sigma \times \{z\}) = \partial(\sigma) \times \{z\}$ defines the boundary maps. In fact this construction is a special case of a cellular (co-)sheaf [11]. Algorithmically it is beneficial that this does *not* require to geometrically construct $\mathbb{R}\mathcal{T}_\epsilon(f)$.

2.2 A census of Betti numbers of real tropical surfaces

We used `mptopcom` [10] to compute regular and full triangulations of $d \cdot \Delta_3$ for $3 \leq d \leq 6$, which are not necessarily unimodular. For $d = 3$ the total number of such triangulations is known to be 21 125 102 [10, Table 3], up to the natural action of the symmetric group S_4 . For higher degrees the corresponding numbers are unknown and probably out of reach for current hard- and software. Still we can compute some of those triangulations, for each degree.

Our experiments suggest that, in order to see many different Betti vectors (b_0, b_1, b_2) , it is preferable to look at many different triangulations. This is feasible for degrees 3 and 4, where we created 1 000 000 and 100 000 orbits of triangulations, respectively. Each of them was equipped with 20 sign distributions which were picked uniformly at random; cf. Figure 3. For $d = 3$ we obtain all values for b_1 which are allowed by (3) if the surface is connected (i.e., $b_0 = 1$).

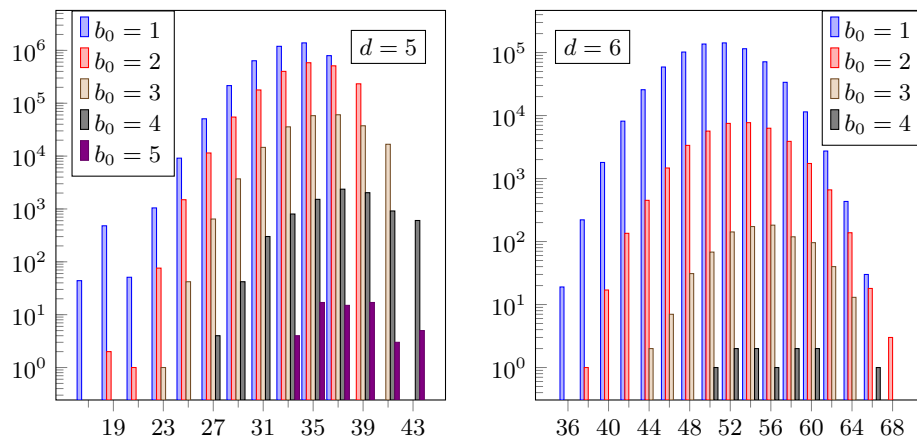


Fig. 4. Distribution of Betti vectors for surfaces of degrees 5 and 6. The colors indicate values for $b_0 = b_2$, the values on the x -axis indicate values for b_1 . For $d = 5$ the most frequent vector is $(1, 35, 1)$ with 21.9%. For $d = 6$ it is $(1, 52, 1)$ with 18.97%.

Additionally, 965 times we saw the Betti vector $(2, 1, 2)$; cf. Example 3. In view of (4) this occurs for non-unimodular triangulations only; all our examples of this kind share the same f -vector $(20, 60, 64, 23)$. For $d = 4$ all the possible Betti vectors occur; cf. (2) and (3).

The case of $d = 5$ turned out to be surprisingly difficult. In our standard setup `mptopcom` quickly produced about a hundred full and regular triangulations before it stalled. `mptopcom`'s algorithm employs a very special search through the flip graph of the point configuration, and it finds all regular triangulations plus some non-regular ones connected by a sequence of flips. Apparently, most neighbors to our first 100 triangulations of $5 \cdot \Delta_3$ are not regular or not full. As we were interested in exploring many different Betti vectors, we created a second sample of triangulations; to this end we employed a random walk on the flip graph of $5 \cdot \Delta_3$. After eliminating multiples, this gave an additional 13 000 regular and full triangulations. On each of the resulting 13 100 triangulations we tried 500 random sign distributions; cf. Figure 4 (left) for the combined statistic. For $d = 6$ we checked 1 500 triangulations with 500 sign distributions each; cf. Figure 4 (right).

No matter how hard we try we will only see a tiny fraction of all possible real tropical surfaces of higher degrees. So the distributions for $d = 5$ and $d = 6$ may not even be close to the “truth”. Yet for $d = 5$ we observed $b_1 = 43$, whereas $b'_1 = 45$; cf. Table 1. We found 61 triangulations of $5 \cdot \Delta_3$ with five components, none of which were unimodular. The maximal number of components in the unimodular case was four. For $d = 6$ our census is way off the theoretical bounds.

3 Implementation in polymake

`polymake` is a comprehensive software system for polyhedral geometry and related areas of mathematics [1]. Mathematical objects like tropical hypersurfaces are determined by their *properties*. Upon a user query the system directly returns a property (e.g., a tropical polynomial or the dual polyhedral subdivision) if this is known, or it computes it by applying a sequence of *rules*. Subsequently, the property asked for becomes known, along with any intermediate results. Throughout the life of such a *big object* the number of properties grows; objects, with their properties, can be saved and loaded again. The latter is useful, e.g., for processing data on a cluster and examining them on a laptop later.

The computation which is relevant here takes a tropical polynomial f (such that the Newton polytope $\mathcal{N}(f)$ is a dilated simplex) and a sign distribution ϵ as input and computes the \mathbb{Z}_2 -Betti numbers of the real part $\mathbb{R}\mathcal{T}_\epsilon(f)$ of the real tropical hypersurface $\mathcal{T}_\epsilon(f)$. The individual steps are: (1) find the maximal cells of $\mathcal{T}(f)$ via a dual convex hull computation; (2) compute the Hasse diagram of the entire face lattice of $\mathcal{T}(f)$; (3) construct the chain complex (5) from that Hasse diagram; (4) compute ranks of the boundary matrices mod 2. Each step is implemented as a separate rule, which makes the code highly modular and reusable. In particular, the only implementation which is really new is step (3).

We wish to give some details about the first two steps. Often the dual convex hull computation is the most expensive part. For this `polymake` has interfaces to several algorithms and implementations, the default being PPL [2] which is also used here. In general, it is difficult to predict which algorithm performs best; see [1] for extensive convex hull experiments. The computation of the Hasse diagram uses a combinatorial procedure whose complexity is linear in the size of the output, i.e., the total number of cells of the tropical hypersurface; cf. [5].

3.1 Running times

To compare the running times of `Viro.sage` and `polymake` for computing the Betti numbers of patchworked hypersurfaces we conducted two experiments, one for Harnack curves and one for surfaces. All computations were carried out on an AMD Phenom II X6 1090T (3.2GHz, 38528 bmips).

For the Harnack curves, where we have just one curve per degree (the cubic case is Example 2), we repeated the same computation ten times each. Figure 5 (left) shows the mean running time depending on the degree. The `Viro.sage` code showed a rather wide variety, while the `polymake` computations gave almost identical running times for each test.

The experiment for the surfaces is slightly different in that both the tropical polynomials (and triangulations) and the sign distributions were varied. For degrees 3, 4, 5, and 6 we took the first 2000, 1000, 100, and 75 triangulations (as enumerated by `mptopcom`), respectively, and measured the running time for 10 random sign distributions each. Figure 5 (right) shows a box plot for each degree. The boxes indicate the 2nd and 3rd quartiles, the whiskers mark the minimum and maximum time measurements, excluding outliers (i.e., measurements whose

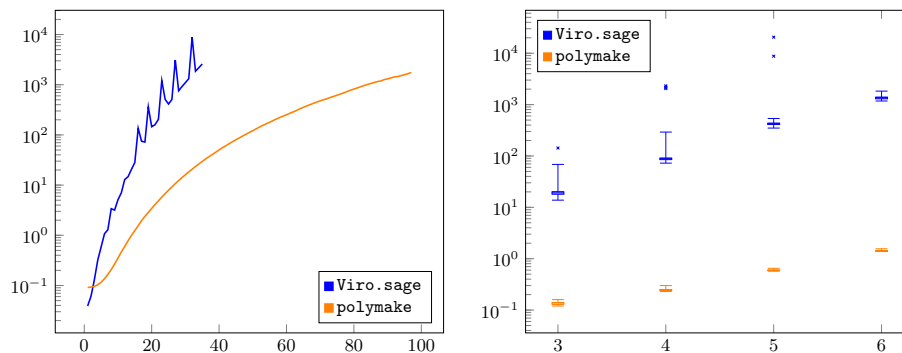


Fig. 5. Time taken to compute Betti numbers (in seconds). Left: Harnack curves, average time by degree. Right: various surfaces, boxplots for each degree.

ratio to the median is either bigger than 4, or smaller than 0.25), which are marked separately. Again `Viro.sage` exhibits a much greater variety of running times than `polymake`.

4 Conclusion

We have shown that our new implementation is capable of determining the \mathbb{Z}_2 -Betti numbers of a patchworked surface of moderate degree within a few seconds. This allows for providing a rich census.

One major reason for `polymake` being faster than `Viro.sage` [18] is that we avoid the explicit construction of a simplicial complex model of $\mathbb{RT}_\epsilon(f)$. Moreover, `polymake` computes \mathbb{Z}_2 Betti numbers directly, while `Viro.sage` goes through a standard homology computation with integer coefficients. `polymake` provides geometric realizations (and integral homology), too, but this is unnecessary here.

References

1. Assarf, B., Gawrilow, E., Herr, K., Joswig, M., Lorenz, B., Paffenholz, A., Rehn, T.: Computing convex hulls and counting integer points with `polymake`. *Math. Program. Comput.* **9**(1), 1–38 (2017)
2. Bagnara, R., Hill, P.M., Zaffanella, E.: The Parma Polyhedra Library: toward a complete set of numerical abstractions for the analysis and verification of hardware and software systems. *Sci. Comput. Programming* **72**(1-2), 3–21 (2008)
3. De Loera, J.A., Rambau, J., Santos, F.: *Triangulations, Algorithms and Computation in Mathematics*, vol. 25. Springer-Verlag, Berlin (2010), structures for algorithms and applications
4. El-Hilany, B., Rau, J., Reneaudineau, A.: Combinatorial patchworking tool. <https://www.math.uni-tuebingen.de/user/jora/patchworking/patchworking.html>

5. Hampe, S., Joswig, M., Schröter, B.: Algorithms for tight spans and tropical linear spaces. *J. Symbolic Comput.* **91**, 116–128 (2019)
6. Itenberg, I.: Topology of real algebraic T -surfaces. vol. 10, pp. 131–152 (1997), real algebraic and analytic geometry (Segovia, 1995)
7. Itenberg, I., Shustin, E.: Critical points of real polynomials and topology of real algebraic T -surfaces. *Geom. Dedicata* **101**, 61–91 (2003)
8. Itenberg, I., Shustin, E.: Viro theorem and topology of real and complex combinatorial hypersurfaces. *Israel J. Math.* **133**, 189–238 (2003)
9. Itenberg, I., Viro, O.: Patchworking algebraic curves disproves the Ragsdale conjecture. *Math. Intelligencer* **18**(4), 19–28 (1996)
10. Jordan, C., Joswig, M., Kastner, L.: Parallel enumeration of triangulations. *Electron. J. Combin.* **25**(3), Paper 3.6, 27 (2018)
11. Kastner, L., Shaw, K., Winz, A.L.: Cellular sheaf cohomology of `polymake`. In: Combinatorial algebraic geometry, Fields Inst. Commun., vol. 80, pp. 369–385. Fields Inst. Res. Math. Sci., Toronto, ON (2017)
12. Maclagan, D., Sturmfels, B.: Introduction to tropical geometry, Graduate Studies in Mathematics, vol. 161. American Mathematical Society, Providence, RI (2015)
13. Renaudineau, A., Shaw, K.: Bounding the Betti numbers of real hypersurfaces near the tropical limit (2019), preprint [arXiv:1805.02030](https://arxiv.org/abs/1805.02030)
14. Viro, O.: Curves of degree 7, curves of degree 8 and the Ragsdale conjecture. *Dokl. Akad. Nauk SSSR* **254**(6), 1306–1310 (1980)
15. Viro, O.: Gluing algebraic hypersurfaces, removing of singularities and constructions of curves. Topology conference, Proc., Collect. Rep., Leningrad 1982, 149–197 (1983). English translation [arXiv:math/0611382](https://arxiv.org/abs/math/0611382).
16. Viro, O.: Gluing of plane real algebraic curves and constructions of curves of degrees 6 and 7. In: Topology (Leningrad, 1982), Lecture Notes in Math., vol. 1060, pp. 187–200. Springer, Berlin (1984)
17. Viro, O.: From the sixteenth Hilbert problem to tropical geometry. *Jpn. J. Math.* **3**(2), 185–214 (2008)
18. de Wolff, T., Kwaakwah, E.O., O’Neill, C.: Viro.sage. <https://cdoneill1.sdsu.edu/viro/> (2018), version 0.4b, posted May 9, 2018